AIAA 80-0138R

Statistical Constraints on Scalar Correlations

Ashok K. Varma,* Guido Sandri,† and Coleman duP. Donaldson‡
Aeronautical Research Associates of Princeton, Inc., Princeton, N.J.

Models for the scalar probability density function (pdf) have to be developed to achieve closure of turbulent transport equations for mixing and reacting flows. The best statistical bounds on a number of moments for two- and three-species flows have been derived and used to construct and test a delta function "typical eddy" pdf model. If has been proven that for two species a rational pdf composed only of delta functions can always be constructed at any point within the statistically valid moment space. The delta function model and a canonical pdf model have been directly compared to experimental pdf measurements and both models show good agreement for higher-order moments, but the delta function model is simpler to construct and is recommended for closure of the transport equations for mixing flows.

Nomenclature

A, A_n	= coefficients of canonical probability density function
p	= pressure
P, P_2, P_λ	= probability functions
R	= universal gas constant
T	= temperature
u	= flow velocity
$W_\alpha, W_\beta, W_\gamma$	= molecular weights of species
x	= coordinate in flow direction
y	= coordinate normal to flow direction
α, β, γ	= species mass fractions
α_3	= model parameter
$\delta(\alpha-\lambda)$	= delta function located at $\alpha=\lambda$
Δ	$= 1-(W_\beta/W_\alpha)$
ϵ_i	= cell sizes in "typical eddy" model
κ	= model parameter
λ	= arbitrary constant
ρ	= density
ρ_*	= normalized density
ψ	= variable

Introduction

MIXING and chemical reactions under turbulent flow conditions are a basic feature of the energy release processes in gas turbine combustors and other propulsion and combustion systems. Any predictive modeling of the flowfield has to properly account for the effects of the turbulence of the flow and its interactions with various physical and chemical processes. There are significant interaction effects of the turbulence on combustion and of the combustion on the turbulence, which are important in determining combustion efficiency, pollutant formation, combustion noise, heat transfer, etc. Second-order closure modeling of turbulent flows provides a convenient framework for studying these interactions and holds promise of providing a reliable predictive computational tool for the design of new systems and improvement of existing combustion systems.

The presence of finite-rate chemical reactions in a turbulent flow introduces the problem of proper modeling of many higher-order correlations involving scalar variables such as concentration, density, and temperature. The transport equations for the mean variables and the second-order correlations are solved in a second-order closure procedure and these equations, especially the chemical reaction source terms, contain many third- and higher-order correlations, such as $\overline{\alpha^2\beta}$, $\overline{\rho^2\alpha}$, $\overline{k\rho\alpha}$, etc. These correlations have to be modeled in terms of the lower-order moments to close the system of transport equations. A convenient procedure for modeling these scalar correlations is to model or calculate the probability density function (pdf) for the scalars.[1-7]

This paper discusses the statistical behavior of scalar variables in turbulent flows. Constraints on two- and three-species systems have been derived. Two proposed models for the pdf, that is, the A.R.A.P. delta function "typical eddy" model[4] and Pope's canonical pdf model,[6] are compared to experimental measurements of the pdf in a two-species mixing layer.

Statistical Constraints on Correlations

Basic statistical principles, such as the Cauchy-Schwarz inequality, Jensen's inequality, Tchebychev's inequality, etc., can be used to develop the set of tightest constraint conditions on correlations of various variables in a turbulent flowfield. The procedure is quite general and can be applied to both scalar and vector variables. At the present time, however, we are mainly interested in developing the constraints for the scalar correlations—specifically those for the species mass fractions (and molar fractions) and density variables. These constraints however, are also applicable to other variables. The mass and molar fractions have upper and lower bounds on moments of all orders, and these are shown later. Both the even and odd moments of the thermodynamic variables (p, T) have the same lower bounds as the mass fractions. In general, the upper bound is infinity, unless a physical constraint is used in the specific problem. The moments of the velocity components have the same lower bounds but only for the even moments.

The constraint conditions are useful in a number of ways in a second-order closure calculation procedure. Two important uses are in checking realizability and in model development.

Realizability

The statistical constraints on first- and second-order correlations are important in the question of realizability of second-order closure turbulence models. A number of recent papers[8-12] have investigated some aspects of this problem. The lower-order moments are calculated by the solution of a set of modeled partial-differential equations. It is possible that the modeled equations may not have solutions that are consistent with the independently derived statistical con-

Presented as Paper 80-0138 at the AIAA 18th Aerospace Sciences Meeting, Pasadena, Calif., Jan. 14-16, 1980; submitted Sept. 30, 1980; revision received Feb. 25, 1981.

*Consultant. Member AIAA.
†Senior Consultant.
‡Senior Consultant. Associate Fellow AIAA.

straints. This will require suitable modifications of the models used in the equations. Furthermore, it is necessary to insure that the initial conditions for the equations are within the allowed moment space.

Development of pdf Model

The constraints on third- and higher-order moments are useful in formulating closure models for these correlations. A popular closure approach is to construct the pdf for the scalar variables. The constraints on the correlations define the entire statistically allowed region, and the pdf model should be checked for validity in this entire space. As will be shown later, the constraints are also useful in determining model-parameter sensitivity and the error bounds of the model, and in comparing the performance of alternate pdf models.

Statistical Constraints for Two Species

Consider a two-species flow at constant pressure and temperature. α and β are the mass fractions of the species. Assume $W_\alpha > W_\beta$. ρ_* is a normalized density,

$$\rho_* = \rho/(W_\beta \bar{p}/R\bar{T}) \qquad p' = T' = 0$$

define

$$\Delta = 1 - (W_\beta / W_\alpha) \qquad 0 \leq \Delta \leq 1$$

$$\rho_* = 1/1 - \Delta\alpha$$

The tightest constraints have been derived using basic statistical theorems.[13,14] The results are summarized below.

$$0 \leq \bar{\alpha} \leq 1 \tag{1}$$

$$\bar{\alpha}^2 < \overline{\alpha^2} < \bar{\alpha} \tag{2}$$

We note that the domain defined by Eq. (2) is significantly tighter than the one obtained by du Vachat.[9] No legitimate pdf can be constructed over the entire domain calculated in Ref. 9. The bounds on $\overline{\alpha^3}$ for given $\bar{\alpha}$ and $\overline{\alpha^2}$ are

$$\overline{\alpha^2}^2/\bar{\alpha} \leq \overline{\alpha^3} \leq \overline{\alpha^2} - (\bar{\alpha} - \overline{\alpha^2})^2/(1-\bar{\alpha}) \tag{3}$$

The bounds on $\overline{\alpha^3}$ if only $\bar{\alpha}$ is specified are

$$\bar{\alpha}^3 < \overline{\alpha^3} < \bar{\alpha} \tag{4}$$

The constraints on $\overline{\rho_*\alpha}$ for given $\bar{\alpha}$ and $\overline{\alpha^2}$ are

$$\frac{\overline{\alpha^2}}{\bar{\alpha} - \Delta\overline{\alpha^2}} < \overline{\rho_*\alpha} \leq \frac{1}{1-\Delta}\,\frac{\bar{\alpha}(1-\bar{\alpha}) - \Delta(\bar{\alpha} - \overline{\alpha^2})}{(1-\bar{\alpha}) - \Delta(\bar{\alpha} - \overline{\alpha^2})} \tag{5}$$

For a two-species system, the complete set of constraints on all moments up to the third-order has been obtained as a function of prescribed lower-order moments. The results show that the higher-order moments are tightly constrained when the lower-order moments are specified. The nature of the constraints can be illustrated by comparing the bounds on $\overline{\alpha^3}$ given by Eqs. (3) and (4), as shown in Fig. 1. The dotted lines are the bounds on $\overline{\alpha^3}$ for given $\bar{\alpha}$. For given $\bar{\alpha}$, we now pick $\overline{\alpha^2}$ at the middle of its allowed range, $\overline{\alpha^2} = (\bar{\alpha} + \overline{\alpha^2})/2$. The solid lines indicate the bounds on $\overline{\alpha^3}$ for specified $\bar{\alpha}$ and $\overline{\alpha^2}$. The important point to be noted is that the bounds on $\overline{\alpha^3}$ when two lower-order moments are specified are significantly narrower than the bounds when only one lower-order moment is specified. If the two lower-order moments are known, the constraints on $\overline{\alpha^3}$ are sufficiently tight to enable us to make a good estimate of its value. This has important implications with regard to the modeling of the scalar pdf, as discussed later in this paper.

Another property of the statistical bounds of importance in modeling is that extremum values of the statistical bounds can only be realized by discrete pdf's, that is, pdf's composed of delta functions. Delta functions are, thus, a necessary component of pdf's. Continuous pdf's alone cannot be valid over the entire moment space. Consider the bounds on $\overline{\alpha^2}$. At the upper bound, $\overline{\alpha^2} = \bar{\alpha}$, and the pdf corresponds to two delta functions located at $\alpha = 0$ and 1,

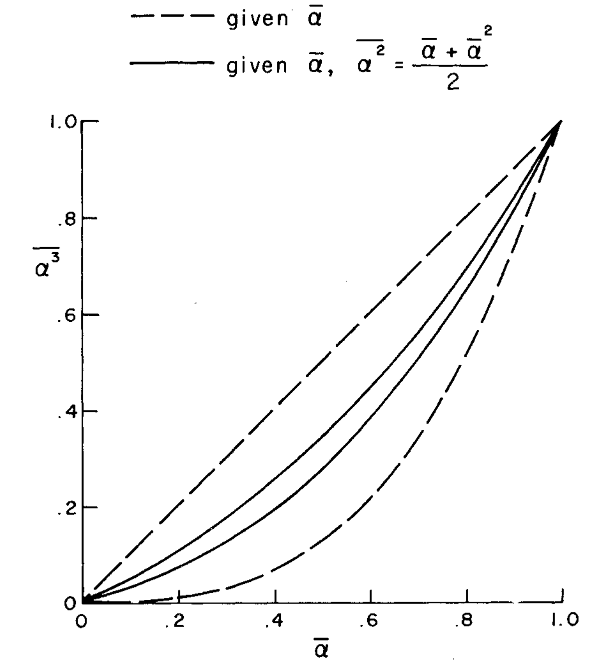

Fig. 1 Comparison of the statistical bounds on $\overline{\alpha^3}$ for specified lower-order moments.

$$P(\alpha) = (1-\bar{\alpha})\delta(\alpha) + \bar{\alpha}\delta(\alpha - 1) \tag{6}$$

At the lower bound, $\overline{\alpha^2} = \bar{\alpha}^2$, and the pdf can be shown to be

$$P(\alpha) = \delta(\alpha - \bar{\alpha}) \tag{7}$$

A popular model for the pdf is a clipped Gaussian.[2] For small fluctuations, this model does approach the limiting pdf corresponding to the lower bound on $\overline{\alpha^2}$. However, it cannot attain the upper-bound pdf corresponding to maximal fluctuations. Ideally, a pdf composed of delta functions and continuous functions will be desirable. We have demonstrated however, that a pdf composed of delta functions alone can always be constructed at every point in the statistically valid moment space. This pdf is simpler to construct than other proposed pdf models, and we will show that it provides sufficient accuracy for closure of the transport equations for turbulent mixing flows of two species.

Statistical Constraints for Three Species

The calculation of the complete set of the bounds for a three-species system becomes very complicated after the first few moments. We have obtained the bounds on some of the species moments of interest in simple reacting flow problems. The results are briefly described below with further discussion available in Refs. 15 and 16. Consider a three-species flow with constant pressure and temperature. α, β, and γ represent the mass fractions of the species.

Given $\bar{\alpha}$ and $\bar{\beta}$

The bounds on second- and third-order correlations given the first-order correlations have been derived. For a three-species system, the allowed phase space region for the pdf is a triangle, as shown in Figs. 2a-c. The specification of $\bar{\alpha}$ and $\bar{\beta}$

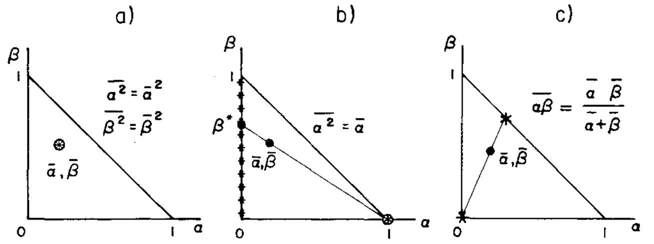

Fig. 2 pdf's for extremum values of second-order moments for specified $\bar{\alpha}$ and $\bar{\beta}$.

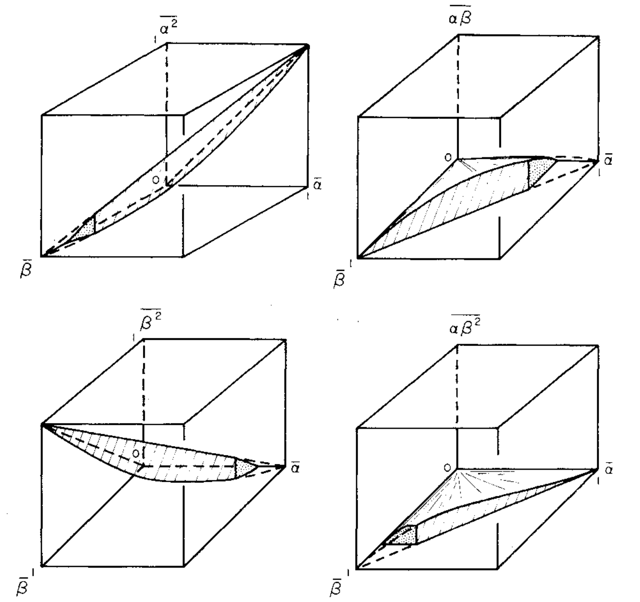

Fig. 3 Statistical constraints on second and third moments for specified $\bar{\alpha}$ and $\bar{\beta}$ in a three-species flow.

corresponds to defining the location of the centroid. The bounds on $\overline{\alpha^2}$ and $\overline{\beta^2}$ are

$$\bar{\alpha}^2 \le \overline{\alpha^2} \le \bar{\alpha} \tag{8}$$

$$\bar{\beta}^2 \le \overline{\beta^2} \le \bar{\beta} \tag{9}$$

Pdf's can be constructed (see Figs. 2a and 2b) that attain these extremum values, and therefore, the above represent the best bounds on the second-order moments. In these figures, the mass locations are depicted by stars. The bounds on $\overline{\alpha\beta}$ are

$$0 \le \overline{\alpha\beta} \le \bar{\alpha}\bar{\beta}/(\bar{\alpha}+\bar{\beta}) \tag{10}$$

The upper bound on $\overline{\alpha\beta}$ (Fig. 2c) is believed to be new and has been confirmed by the method of induction considering an arbitrarily large number of point masses.[16] The bounds on $\overline{\alpha\beta^2}$ are the smaller of the following three

$$0 \le \overline{\alpha\beta^2} \le \bar{\alpha}\bar{\beta}/(\bar{\alpha}+\bar{\beta})$$

$$0 \le \overline{\alpha\beta^2} \le \bar{\alpha} - 2\bar{\alpha}^2 + \bar{\alpha}^3$$

$$0 \le \overline{\alpha\beta^2} \le \bar{\beta}(1-\bar{\beta}) \tag{11}$$

The best bounds on the correlations in $(\bar{\alpha},\bar{\beta})$ space are shown in Fig. 3. It should be noted that very small regions of the unit cube are allowed.

Given $\bar{\alpha}$, $\bar{\beta}$, and $\overline{\alpha^2}$

We have also determined the allowed regions for $\overline{\beta^2}$, $\overline{\alpha\beta}$, and $\overline{\alpha\beta^2}$ in $\overline{\alpha^2}$ space for specified $\bar{\alpha}$ and $\bar{\beta}$. The independent

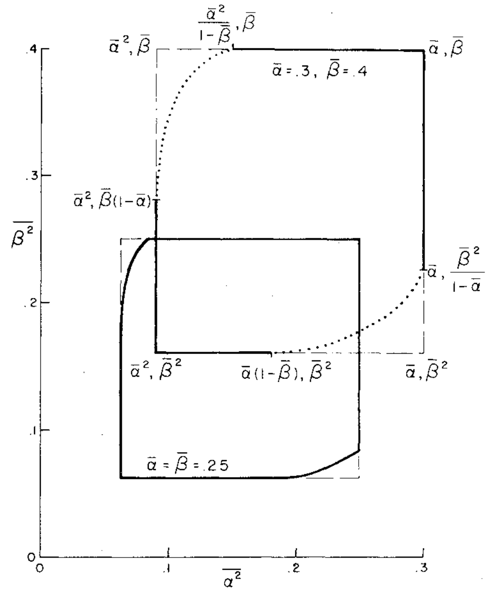

Fig. 4 Statistical bounds on $\overline{\beta^2}$ and $\overline{\alpha^2}$ for specified $\bar{\alpha}$ and $\bar{\beta}$ in a three-species system.

bounds on $\overline{\alpha^2}$ and $\overline{\beta^2}$ [Eqs. (9) and (10)] define a rectangle in $(\overline{\alpha^2}, \overline{\beta^2})$ space. However, there are regions within the rectangle that must be excluded due to the specification of one of the moments. For example, if $\overline{\alpha^2}$ is minimal, $\overline{\beta^2} \le \bar{\beta}(1-\bar{\alpha}) < \bar{\beta}$. Details of the proofs are available in Ref. 16. Figure 4 shows the results for the bounds in $(\overline{\alpha^2}, \overline{\beta^2})$ space for two sets of values of $\bar{\alpha}$ and $\bar{\beta}$. The connecting curves between the allowed points on the boundaries have been determined by considering a series of pdf's consisting of two delta functions located on the sides of the triangle. Some of the curves still have to be calculated, but their expected behavior is shown by dotted lines. We believe that these represent the best bounds on the moments, but a general proof for all mass distributions is not yet available. Figures 5 and 6 show the corresponding results for the allowed regions in $(\overline{\alpha^2}, \overline{\alpha\beta})$ and $(\overline{\alpha^2}, \overline{\alpha\beta^2})$ space. As in the case of the bounds on the third moment for a two-species system, the important feature to note here is the tightness of the constraints. For specified lower-order moments, $\bar{\alpha}$, $\bar{\beta}$ and $\overline{\alpha^2}$, $\overline{\alpha\beta^2}$ has a maximum value of order 0.1. For three species we have not yet investigated the constraints when second-order moments involving the density are also specified, but this will lead to further tightening of the bounds on the third-order moments of interest.

Models for Probability Distribution Functions

The A.R.A.P. delta function "typical eddy" pdf model and a canonical continuous function pdf model[6] have been directly compared to experimental measurements. The two pdf models are briefly described below. We will attempt to demonstrate that the delta function model provides sufficient accuracy for closure of the transport equations for turbulent mixing flows. The results obtained from the two models are quite comparable, but the delta function model is simpler to construct than the canonical model.

"Typical Eddy" pdf Model

The "typical eddy" model is an attempt to construct the joint pdf for the scalar variables by using all the available information from a second-order closure analysis. The model may consist of combinations of delta functions and continuous functions, but, for the present, we have studied a model composed only of delta functions. The pdf model structure is assumed, and the model parameters are determined by matching the moments of the model to the values of the correlations obtained from the solution of the transport equations. The procedure is detailed in Refs. 4 and 14.

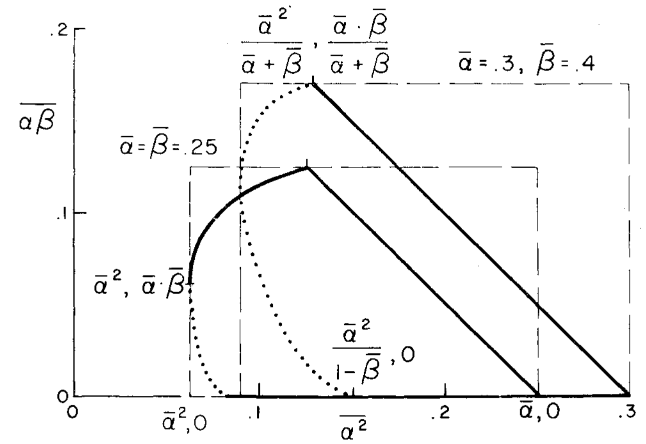

Fig. 5 Statistical bounds on $\overline{\alpha\beta}$ and $\overline{\alpha^2}$ for specified $\bar{\alpha}$ and $\bar{\beta}$ in a three-species system.

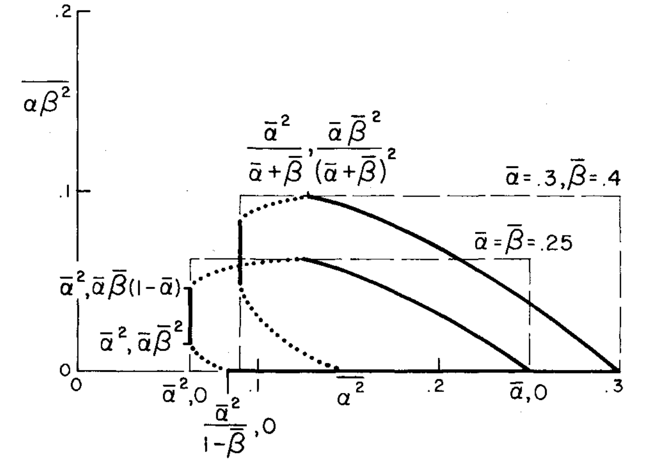

Fig. 6 Statistical bounds on $\overline{\alpha\beta^2}$ and $\overline{\alpha^2}$ for specified $\bar{\alpha}$ and $\bar{\beta}$ in a three-species system.

The delta function "typical eddy" models for two-species flows are shown in Fig. 7. For constant density flows, the model has three delta functions, while for variable density flows the model consists of four delta functions. The ϵ_i are probabilities of occurrence of the indicated species mixtures. The model has one free parameter, α_3. We have demonstrated[14] that the allowed range of α_3 corresponds directly to the statistical bounds on the third-order moments. With the parameter α_3 selected at any point within its allowed range, we have also shown that a physically correct pdf model (positive strength delta functions with locations between 0 and 1) can be constructed at *every* point in the statistically valid moment space.

Canonical pdf Model

Pope[6] has proposed a general model for joint pdf's of scalar variables that is based on the concept of maximizing the entropy of information. If the first λ moments of the pdf are known, then the most likely value of the pdf $P_\lambda(\psi)$ is

$$P_\lambda(\psi)=\exp\sum_{n=0}^{\lambda}A_n\psi^n \tag{12}$$

The $\lambda+1$ coefficients A_n are presumably uniquely determined from the λ moments and the condition that P integrates to unity.

For second-order closure of constant density flows, the canonical model has the form

$$P_2(\alpha)=\exp(A_0+A_1\alpha+A_2\alpha^2) \tag{13}$$

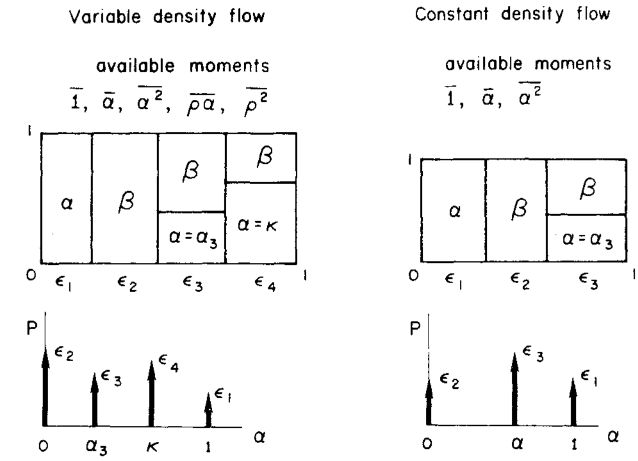

Fig. 7 Delta function "typical eddy" model structures for two-species flows.

where A_0, A_1, and A_2 are determined from values of the moments 1, $\bar{\alpha}$, and $\overline{\alpha^2}$. The construction of the model requires a two-dimensional parameter search involving integral relations. For variable density flows, the second-order closure procedure provides information on five moments—1, $\bar{\alpha}$, $\overline{\alpha^2}$, $\overline{\rho_*\alpha}$, $\overline{\rho_*^2}$—and the construction of the canonical model will involve a four-dimensional search for the parameters. This is conceptually straightforward but requires a significant computational effort and is quite a bit more complicated than the construction of the delta function model which involves the solution of algebraic equations. The comparisons of the two pdf models will be limited to constant density flows.

Comparison of pdf Models with Experiments

Konrad[17] has made a series of detailed measurements of the pdf in low-speed, constant and variable-density shear layer flows of two species. The measurements consist of mean velocity, mean concentration, concentration fluctuation correlations, species intermittency functions, and the species pdf's. The latter two measurement parameters are used for the direct pdf model comparisons.

The pdf measurements of Konrad are used to determine the values of the lower-order moments—$\bar{\alpha}$ and $\overline{\alpha^2}$ for constant density, and $\bar{\alpha}$, $\overline{\alpha^2}$, $\overline{\rho_*\alpha}$, and $\overline{\rho_*^2}$ for variable density—that are needed to construct the delta function and canonical pdf models. The measured pdf is also used to calculate experimental values of a number of third-order correlations of interest, such as $\overline{\alpha\beta^2}$. The third-order correlations are also computed from the model pdf's, and the results compared to the measurements.

Constant Density Shear Layer Flow

The predictions of the third-order moment $\overline{\alpha\beta^2}$ by the model are compared to the experimental measurements in Fig. 8. The ordinate of the figure is $\overline{\alpha\beta^2}_{\rm model}/\overline{\alpha\beta^2}_{\rm expt}$. The abscissa is the normalized coordinate across the shear layer. The thin dotted lines show the upper and lower bounds on the third-order moment. Several choices for the selection of the free parameter α_3 in the delta function pdf model were explored, for example, $\alpha_3=\bar{\alpha}$, α_3 corresponding to minimum entropy of mixing, α_3 at midrange, etc.[14] The best results are obtained for α_3 at the middle of the allowed range and these are shown in the figure along with the predictions for the third-order moment obtained from the canonical pdf model. It can be seen that the results of the two models are comparable. The delta function model, however, is simpler to construct than the canonical model even when just two moments are specified.

Figure 9 compares the model predictions for species intermittency or the probability of finding pure species at various points across the flowfield. The predictions and the

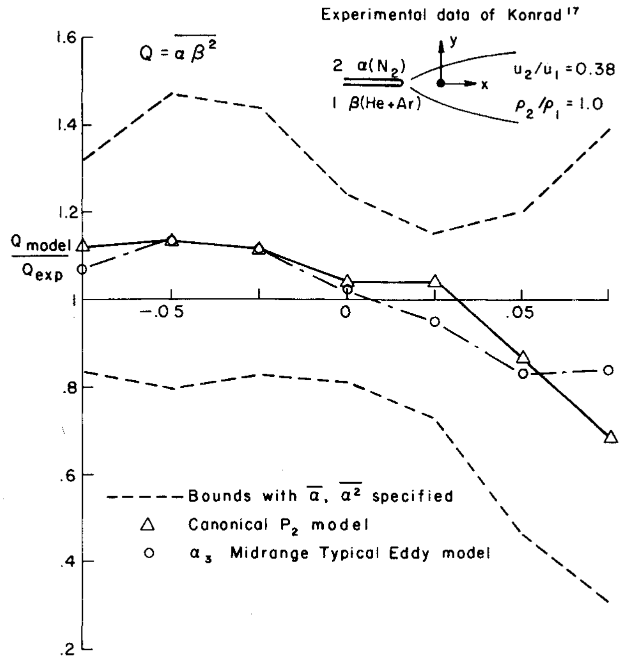

Fig. 8 Comparison of model predictions and experiments for the third moment $\overline{\alpha\beta^2}$; constant density shear layer.

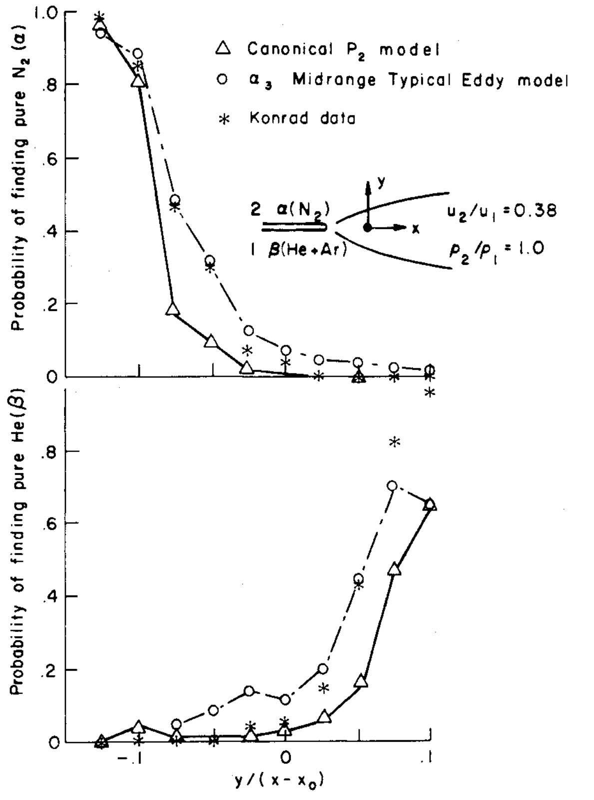

Fig. 9 Comparison of model predictions with experiments for the species intermittency; constant density shear layer.

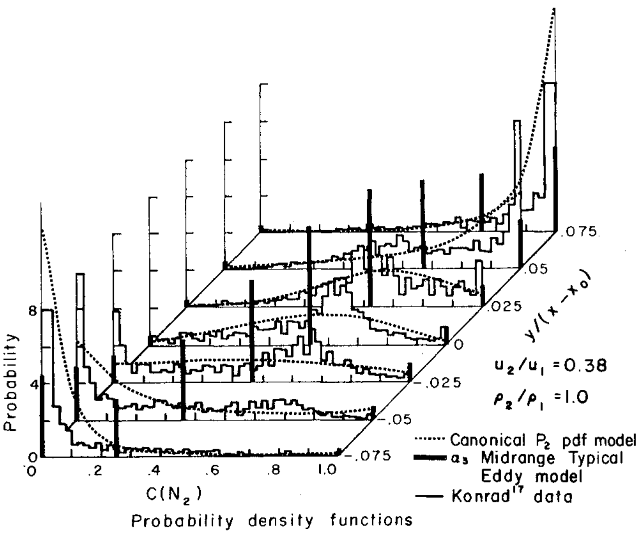

Fig. 10 Comparison of canonical pdf model and delta function pdf model with measured pdf.

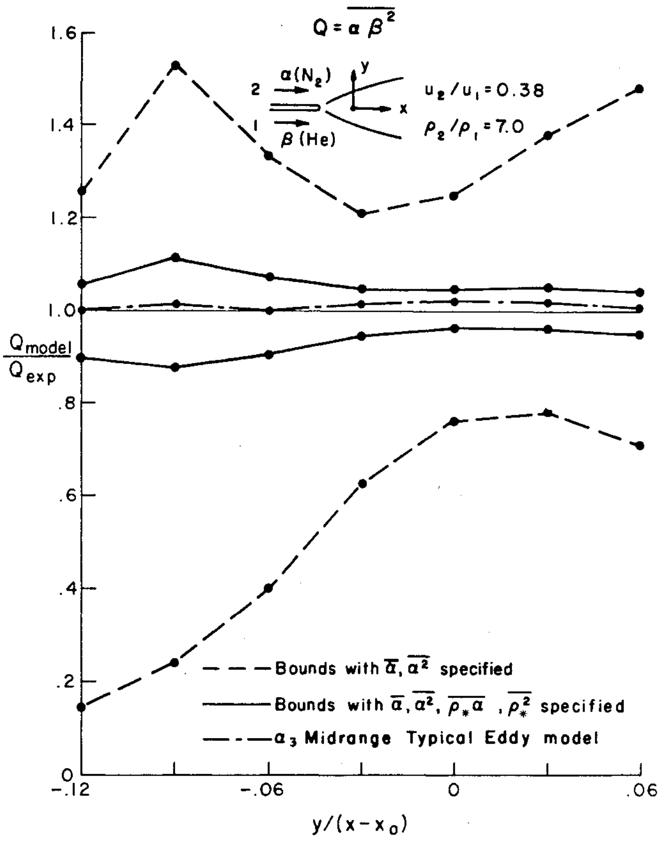

Fig. 11 Comparison of model predictions with experiments for the third moment $\overline{\alpha\beta^2}$; variable density shear layer.

measurements used a 3% cutoff value, that is, the probability of the pure species α was taken to be the integral of the pdf from $\alpha = 1$ to $\alpha = 0.97$. The results show that the delta function pdf model does a somewhat better job of predicting the species intermittency than the canonical model.

The canonical P_2 pdf model and the delta function pdf for α_3 at midrange value are compared to the experimental pdf in Fig. 10. The construction of the canonical model required a significant effort and we expected the model to do better than it does. The canonical model misses many details of the experimental pdf and smears out the peaks. The results for the delta function model show the delta functions at the predicted locations in the concentration space. The absolute magnitude of the strengths of the delta functions cannot be directly plotted on this graph, and we have selected a convenient scale for depicting the relative strengths of the delta functions. The strengths and locations of the delta functions seem to follow the features of the experimental pdf structure. Obviously, due to the continuous nature of the canonical model, it does better visually than the delta function model, but the latter is much simpler to construct and it does a very adequate job of predicting the higher-order moments and species intermittency.

Variable Density Shear Layer Flow

The predictions of the third-order moment $\overline{\alpha\beta^2}$ by the delta function pdf model are compared to the experimental data in Fig. 11. The canonical pdf model was not computed for this flow. The dotted lines in the figure show the upper and lower bounds on the third moment when only two lower-order moments are used for the model construction. In this case, $\overline{\alpha\beta^2}$ has a broad range of possible values, and some models within the statistical range can lead to significant errors compared to the experiment. However, when four lower-order moments are specified, the model values of $\overline{\alpha\beta^2}$ are tightly constrained as shown by the solid lines. In the case of the delta function "typical eddy" model, the solid lines correspond to the entire valid range of the free parameter α_3. It can be seen that with any choice of α_3 within this range, it is possible to predict $\overline{\alpha\beta^2}$ (and other third-order moments) to better than 10% accuracy. This is significantly better accuracy than the expected error bounds on experimental measurements of third-order moments. The delta function "typical eddy" model can be used to provide even better accuracy by empirically selecting the parameter α_3 at the middle of its allowed range, as shown in the figure. The third moment can now be predicted to better than 2% accuracy across the entire flowfield.

It must be noted that the statistical constraints on the moments are independent of the pdf model. Any and all statistically valid pdf models that match the given values for the lower-order moments will predict values for the third moment within these same bounds. These other models will typically be more difficult to construct and may not lead to significantly better prediction of third-order moments. The comparison of the canonical and delta function pdf models for constant density flows discussed earlier illustrated this very point.

Conclusions

The direct comparison of the delta function "typical eddy" pdf model for two species with pdf measurements has demonstrated that this simple model gives adequate agreement with measurements of higher-order correlations and species intermittency.

The complete set of statistical constraints on correlations for two-species flow has been derived. The constraints have been used to prove that delta functions are a necessary part of the pdf in order to attain the extremum values of the moments. A rational pdf composed of a set of delta functions alone can always be constructed anywhere within the statistically valid moment space. A pdf of this type, when constructed using all of the information in a second-order closure calculation, can predict the higher-order correlations to better accuracy than they can be measured. Therefore, it appears unnecessary to construct more complex pdf's for the purpose of closure of the turbulence equations for mixing flows.

A number of important statistical constraints for three-species systems have been derived. These indicate that the third-order correlations are again quite tightly constrained and, therefore, it appears likely that the conclusions arrived at for two-species mixing flows will also be applicable to simple reacting flows.

Acknowledgments

This research effort has been supported by the Office of Naval Research under Contract Nos. N00014-75-C-1143 (Project SQUID) and N00014-79-C-0335. Some support from the U.S. Air Force Office of Scientific Research under Contract No. F44620-76-C-0048 is also gratefully acknowledged. The authors wish to acknowledge the close involvement of Dr. P. J. Mansfield in the derivation of the statistical bounds.

References

[1] Bray, K.N.C. and Moss, J. B., "A Unified Statistical Model of the Premixed Turbulent Flame," AASU Rept. No. 335, University of Southampton, Dept. of Aeronautics and Astronautics, Southampton, England, Nov. 1974.

[2] Lockwood, F. C. and Naguib, A. S., "The Prediction of the Fluctuations in the Properties of Free, Round-Jet, Turbulent, Diffusion Flames," *Combustion and Flame*, Vol. 24, 1975, p. 109.

[3] Bonniot, J. C., Borghi, R., and Magre, P., "Turbulent Combustion in a Stirred Combustor," *AIAA Progress in Astronautics and Aeronautics, Turbulent Combustion*, Vol. 58, edited by L. A. Kennedy, AIAA, New York, 1977, pp. 331-350.

[4] Donaldson, C. duP. and Varma, A. K., "Remarks on the Construction of a Second-Order Closure Description of Turbulent Reacting Flows," *Combustion Science and Technology* (special issue on Turbulent Reactive Flows), Vol. 13, 1976, pp. 58-78.

[5] Pope, S. B., "The Probability Approach to the Modeling of Turbulent Reacting Flows," *Combustion and Flame*, Vol. 27, 1976, p. 299.

[6] Pope, S. B., "Probability Distributions of Scalars in Turbulent Shear Flows," *Proceedings of the Second Symposium on Turbulent Shear Flows*, Imperial College, London, United Kingdom, July 1979.

[7] Spalding, D. B., "A General Theory of Turbulent Combustion: The LaGrangian Aspects," AIAA Paper 77-141, 1977.

[8] Lumley, J. L., "On Third-Order Mixed Moments," *Physics of Fluids*, Vol. 17, 1974, p. 1127.

[9] du Vachat, R., "Realizability Inequalities in Turbulent Flows," *Physics of Fluids*, Vol. 20, 1977, p. 551.

[10] Schumann, V., "Realizability of Reynolds-Stress Turbulence Models," *Physics of Fluids*, Vol. 20, 1977, p. 271.

[11] Kraichnan, R., "Vibrational Method in Turbulence Theory," *Physical Review Letters*, Vol. 42, 1979, p. 1263.

[12] Kraichnan, R., "Realizability Inequalities and Closed Moment Equations," *Proceedings of the International Conference on Nonlinear Dynamics*, New York, 1979; to appear in the *Annals of the New York Academy of Sciences*.

[13] Ahiezer, N. I. and Krein, M., *Some Questions in the Theory of Moments*, American Mathematical Society, Providence, R.I., 1962.

[14] Sandri, G., Mansfield, P. J., Varma, A. K., and Donaldson, C. duP., "Statistical Constraints on Scalar Variables in Turbulent Flows," A.R.A.P. Rept. No. 346, Aeronautical Research Associates of Princeton, Inc., Princeton, N.J., Aug. 1978, prepared for the U.S. Air Force Office of Scientific Research.

[15] Varma, A. K., Sandri, G. and Donaldson, C. duP., "Second-Order Closure Modeling of Turbulent Mixing and Reacting Flows," AGARD-CP-275, *Proceedings of Propulsion and Energetics Panel 54th (B) Specialists' Meeting on Combustor Modelling*, DFVLR, Cologne, Germany, Oct. 1979.

[16] Varma, A. K., Mansfield, P. J., and Sandri, G., "Second-Order Closure Modeling of Variable Density Turbulent Flows," Office of Naval Research, Project SQUID Tech. Rept. ARAP-2-PU, 1979.

[17] Konrad, J. H., "An Experimental Investigation of Mixing in Two-Dimensional Turbulent Shear Flows with Applications to Diffusion-Limited Chemical Reactions," Office of Naval Research, Project SQUID Tech. Rept. CIT-8-PU, 1976.